

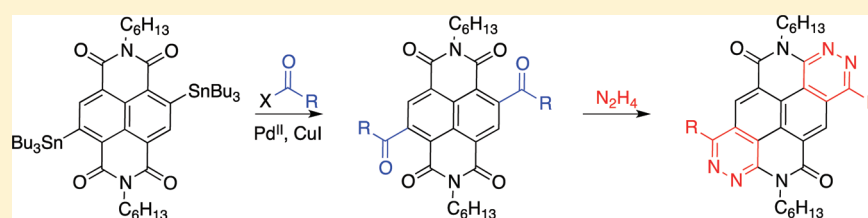
2,6-Diacylnaphthalene-1,8:4,5-Bis(dicarboximides): Synthesis, Reduction Potentials, and Core Extension

Lauren E. Polander,[†] Laxman Pandey,[†] Alexander Romanov,[‡] Alexandr Fonari,[‡] Stephen Barlow,[†] Brian M. Seifried,[†] Tatiana V. Timofeeva,[‡] Jean-Luc Brédas,[†] and Seth R. Marder^{*,†}

[†]School of Chemistry and Biochemistry, Center for Organic Photonics and Electronics, Georgia Institute of Technology, Atlanta, Georgia 30332-0400, United States

[‡]Department of Chemistry, New Mexico Highlands University, Las Vegas, New Mexico 87701, United States

S Supporting Information



ABSTRACT: 2,6-Diacyl derivatives of naphthalene-1,8:4,5-bis(dicarboximide)s have been synthesized via Stille coupling reactions of the corresponding 2,6-distannyl derivative with acyl halides. Reaction of these diketones with hydrazine gave phthalazino[6,7,8,1-*lmna*]pyridazino[5,4,3-*gh*][3,8]phenanthroline-5,11(4*H*,10*H*)-dione fused-ring derivatives. The products were characterized by UV–vis absorption spectroscopy and electrochemistry, modeled using density functional theory calculations, and, in some cases, studied and compared using single-crystal X-ray diffraction.

INTRODUCTION

Rylene diimide derivatives, particularly naphthalene and perylene diimides (NDIs and PDIs, respectively), are extensively studied as building blocks in optoelectronic devices, such as field-effect transistors (OFETs),^{1,2} photovoltaic cells (OPVs),^{3–5} dye lasers,⁶ optical switches,⁷ and photodetectors,⁸ as electron acceptors for studying photoinduced energy- and electron-transfer processes^{9–11} and as ligands in nucleic acid studies of telomerase inhibition in metastatic cancer cells.^{12,13} Interest in rylene diimides for these applications stems from their thermal, chemical, and photochemical stability, large electron affinities (EAs), large charge-carrier mobility values, and the ability to tune their electronic properties through well-established organic chemistry.^{1,14}

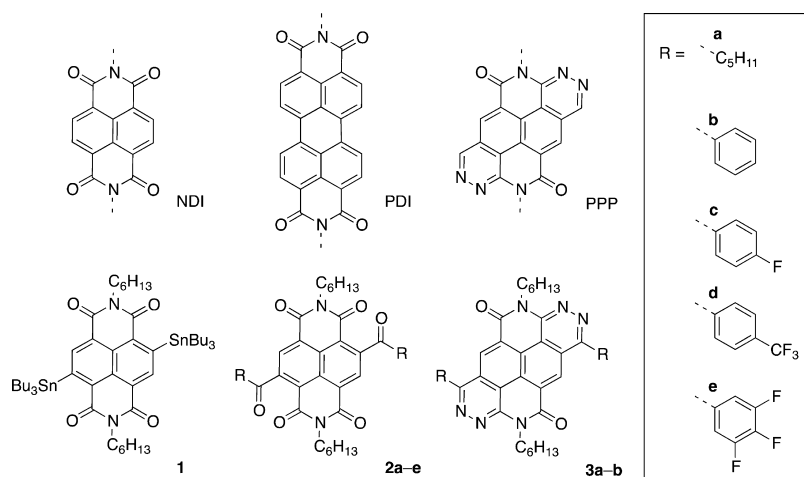
Recently, many groups have focused on tuning the electronic properties and solid-state interactions of these rylene cores to achieve improved charge-carrier stability under ambient conditions, energy-level alignment with suitable electrodes, and specific solid-state molecular packing demonstrating stacking between aromatic systems.^{15–20} The electronic properties of NDI, in particular, have been successfully tuned via core substitution, which typically has a much more significant effect on the redox potentials than variation of the *N,N'*-substituents (a consequence of the presence of nodes on the N atoms in both HOMO and LUMO wave functions), and via extension of the aromatic core system. Core-functionalized NDIs have been synthesized from brominated NDIs, either through nucleophilic substitutions to afford amino, thiol, or alkoxy derivatives,^{21,22} or through Pd-catalyzed coupling reactions to yield cyano,^{23,24} phenyl,^{24,25} alkynyl,²⁴ and thienyl^{25–27} products. Derivatives

have been obtained with reduction potentials ranging from -0.40 to -1.49 V versus $\text{FeCp}_2^{+/0}$ ($\text{Cp} = \eta^5\text{-cyclopentadienyl}$) for a 2,6-dicyano-NDI²³ and a 2,6-dipyrrolidino-NDI,²⁴ respectively. So-called core-expanded NDIs, in which additional rings are fused to a NDI core, have been reported: Hu et al. used the reaction of tetrabromo-NDI with dithiines and dithiolylenes, with the first reduction potentials of these core-expanded NDIs ranging from -0.52 to -0.67 V versus $\text{FeCp}_2^{+/0}$.²⁸ However, core-metalated NDIs that could be used to broaden the scope of NDI chemistry and to yield a wide variety of new NDI products were, until the recent synthesis of 2,6-distannyl-NDIs,²⁹ unknown.

Mono- or diketones obtained by acylation of the NDI core may be of interest due to the influence of the electron-withdrawing acyl moieties on the reduction potential; moreover, use of different alkanoyl or aroyl groups may allow this reduction potential to be tuned. The electron-poor nature of NDIs, however, means direct acylation of the core by Friedel–Crafts methods is impractical. On the other hand, our recent synthesis of 2,6-distannyl-NDIs²⁹ offer the possibility of using the well-known palladium-catalyzed Stille coupling of aryl-stannanes with acyl halides.³⁰ Here, we describe the use of a 2,6-distannyl NDI derivative (**1**)²⁹ to synthesize hitherto unreported 2,6-diacyl-NDIs (**2a–e**), their reaction with hydrazine to yield planar fused-ring 1,7-dialkyl (**3a**) or 1,7-diaryl (**3b**) phthalazino[6,7,8,1-*lmna*]pyridazino[5,4,3-*gh*][3,8]-phenanthroline-5,11(4*H*,10*H*)-diones (PPPs), the optical and

Received: March 26, 2012

Published: May 23, 2012

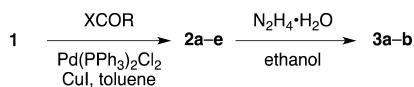


electronic properties of these new classes of compounds (**2a–e**, **3a** and **3b**), and crystal structures of representative examples (**2b**, **3a** and **3b**).

RESULTS AND DISCUSSION

Synthesis. Commercially available alkanoyl and aroyl R groups were chosen to investigate the possibility of obtaining diacyl NDIs by Stille coupling of distannyl NDIs and acyl halides. As noted above, acylation is anticipated to result in anodically shifted reduction potentials; in order to gauge the extent to which the substituents of the aroyl groups may be used to lead to even more facile reduction, aroyl groups with varied degrees of fluorination were used. *N,N'*-Di(*n*-hexyl)-2,6-bis(tri(*n*-butyl)stannyl)naphthalene-1,8:4,5-bis(dicarboximide),²⁹ **1**, was converted using Pd(PPh₃)₂Cl₂, CuI, and the appropriate acylhalide, XCOR (X = Cl, Br), under Stille conditions to *N,N'*-bis(*n*-hexyl)-2,6-diaclynaphthalene-1,8:4,5-bis(dicarboximide) derivatives, **2a–e**, in 26–32% yield (Scheme 1).

Scheme 1. Preparation of **2a–e**, **3a** and **3b**



Hydrazine hydrate has been used extensively in the literature in reactions with 1,2-diacyl-ethylene derivatives to form pyridazine derivatives;^{31,32} this chemistry was applied to the synthesis of new fused-ring structures. 1,7-Di(*n*-pentyl)-4,10-di(*n*-hexyl)phthalazino[6,7,8,1-*lmna*]pyridazino[5,4,3-*gh*][3,8]-phenanthroline-5,11(4*H*,10*H*)-dione, **3a**, and 1,7-di(*n*-phenyl)-4,10-di(*n*-hexyl)phthalazino[6,7,8,1-*lmna*]pyridazino[5,4,3-*gh*][3,8]phenanthroline-5,11(4*H*,10*H*)-dione, **3b**, were synthesized from **2a** and **2b**, respectively, via condensation with hydrazine hydrate in ethanol at reflux (Scheme 1) and were isolated in 35–37% yield.³³ This condensation reaction was not performed on compounds **2c–e** because of poor solubility associated with these compounds under the reaction conditions. The new compounds were characterized by ¹H, ¹⁹F, and, with the exception of the very poorly soluble **2d** and **2e**, ¹³C{¹H} NMR spectroscopy, high-resolution mass spectrometry, and elemental analysis.

DFT Molecular Geometry and Frontier Orbitals. The neutral ground-state structures were obtained at the DFT (B3LYP/6-31G**) level for NDI, **2a–e**, PPP, **3a** and **3b** with all *N,N'*-alkyl groups replaced by methyl groups and, for **2a** and **3a**,

R = C₅H₁₁ replaced by ethyl groups to reduce computational cost. Compounds **2** are characterized by a planar core with a large torsion angle between the plane of the NDI core and the planes containing the ketone functional groups (on average 71° and 76° for alkyl and aryl ketone, respectively); this is mainly due to steric interactions between the C=O and alkyl/aryl groups of the ketone functionalities with the C=O of the NDI imides. As a result, any influence of the acyl substituents on the electronic properties of the core is primarily inductive in nature. Compounds **3a** and **3b**, on the other hand, are characterized by a planar fused core. The phenyl group of **3b** is (on average) estimated to be twisted some 40° out-of-plane with respect to the central core, consistent with the effects of steric interactions between hydrogen atoms in its *ortho*-position with the hydrogen atoms on the core.

The B3LYP/6-31G** HOMO and LUMO wave functions are illustrated for NDI, **2a–e**, PPP, **3a** and **3b** in Figure 1. The HOMO wave functions of **2c** and **2d** are strongly localized on the C(O)R segments, while those for **2a**, **2b**, and **2e**, although still significantly keto-based, are also characterized by partial delocalization onto the core of the NDI. The LUMO wave functions, on the other hand, are strongly localized on the core for all derivatives. The LUMO energy of **2a** is stabilized relative to that of an isolated NDI, a consequence of the inductive withdrawing effect of the acyl substituents. The fluoro- and trifluoromethyl-substituted benzoyl species **2c–e** have still lower LUMO energies, that of **2d** being ca. 0.45 eV lower than that of the parent NDI (Table S1, Supporting Information).

The HOMOs of the PPP systems, **3a** and **3b**, in contrast to those of the acyl derivatives, are π orbitals delocalized over the fused-ring system, with that of **3b** being more extensive than that of **3a** or an unsubstituted PPP because of additional delocalization onto the phenyl substituents. The LUMO wave functions for **3a** and **3b** are similar to one another and to that of the unsubstituted PPP. The HOMO and LUMO energies are destabilized relative to those of an NDI without core substitution by ca. 0.5–1.0 and 0.3 eV, respectively (Figure 1, Table S1, Supporting Information), because of a combination of the reduced electronegativity of nitrogen versus oxygen and of the antibonding interaction between the naphthalene segment and the C=N portions of the phenazine rings that are derived from the acyl groups.

Optical Properties and Electrochemistry. Electronic absorption spectra of *N,N'*-bis(*n*-hexyl) naphthalene diimide (NDI6), **2a–e**, **3a** and **3b** were recorded in dilute dichloromethane solution (ca. 10^{−5} M). Representative spectra are shown in Figure 2; the corresponding absorption maxima and molar absorptivities are summarized in Table 1. The spectra of **2c–e** are

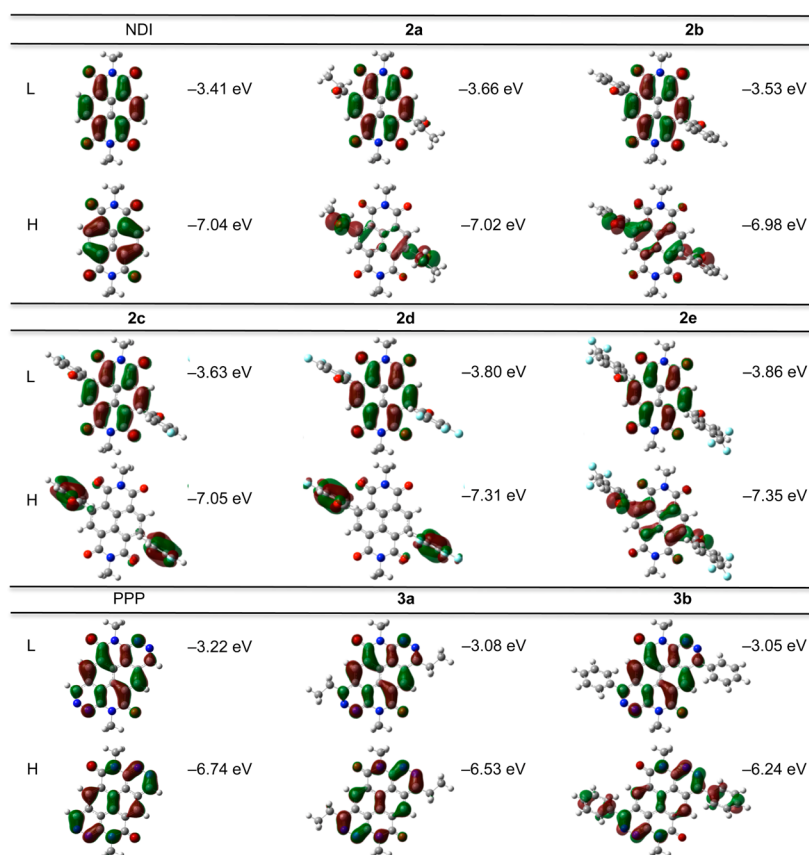


Figure 1. Pictorial representations of the HOMO (H) and LUMO (L) wave functions for N,N' -dimethyl derivatives of NDI, **2a** ($R = C_2H_5$), **2b–e**, PPP, **3a** ($R = C_2H_5$), and **3b**, as determined at the B3LYP/6-31G** level of theory (isovalue surface 0.03 a.u.).

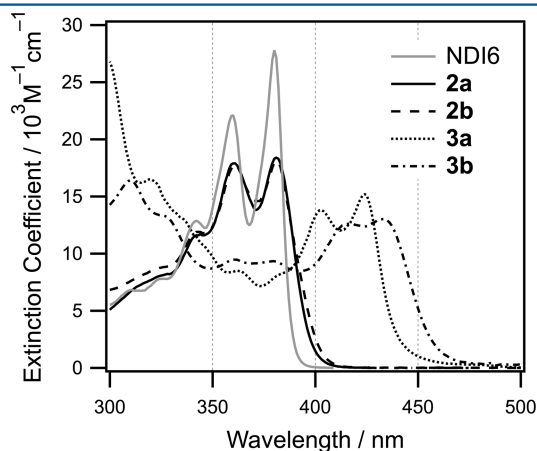


Figure 2. Representative UV-vis spectra of NDI6, **2a**, **2b**, **3a** and **3b** in dilute dichloromethane solutions.

essentially identical to that of **2a** and **2b** and are shown in Figure S1, Supporting Information. The absorption spectra of **2a–e** exhibit prominent vibronically structured absorption bands with maxima at 380–381 nm, similar to that of the corresponding NDI derivative (NDI6, 380 nm). Fluorination of the phenyl moiety does not significantly affect the spectra, which is consistent with all the acyl groups acting primarily as inductively electron-withdrawing substituents.

The absorption spectra of **3a** and **3b** exhibit prominent absorption bands with maxima at 423 and 433 nm, respectively. The absorption maxima of **3a** and **3b** are bathochromically shifted by ca. 50–80 nm relative to that of NDI6 and the diacyl-NDI analogues **2a–e**.

Table 1. Absorption Maxima (nm) and Absorptivities ($10^4 M^{-1} cm^{-1}$) for the Strong UV-vis Absorptions of **2** and **3** in Dichloromethane along with Thin-Film Absorption Maxima (nm), Electrochemical Potentials (V vs $FeCp_2^{+/0}$)^a and DFT Estimates of Electron Affinity and Reorganization Energy (eV)^b

cmpd	λ_{max}		ϵ_{max}	$E_{1/2}^{0/-}$	$E_{1/2}^{-/2-}$	$EA_{adi}(g)^c$	λ_e^d
	soln	film					
NDI6 ^e	380	393	2.76	-1.13	-1.70	-2.03	0.336
2a	380	401	1.79	-0.90	-1.34	-2.45	0.432
2b	380	386	1.88	-0.87	-1.32	-2.40	0.452
2c	381	<i>f</i>	<i>f</i>	-0.84	-1.28	-2.50	0.464
2d	381	<i>f</i>	<i>f</i>	-0.80	-1.26	-2.69	0.470
2e	381	<i>f</i>	<i>f</i>	-0.78	-1.24	-2.74	0.477
3a	423	444	1.52	-1.40	-1.91	-1.83	0.271
3b	433	443	1.30	-1.30	-1.73	-1.91	0.276

^aCyclic voltammetry in $CH_2Cl_2/0.1 M$ nBu_4NPF_6 . ^bSCF values for isolated molecules. ^cAdiabatic EA = SCF energy difference between the relaxed ground-state anion and the ground-state neutral species (obtained for structures in which the alkyl groups are all replaced by methyl groups at the B3LYP/6-31G** level). ^dInternal reorganization energies for $M_A^- + M_B = M_A + M_B^-$ obtained as sum of the SCF energy difference between anion at the neutral geometry and at anion geometry and that between the neutral species at anion geometry and at neutral geometry. ^e N,N' -bis(*n*-hexyl) naphthalene diimide. ^fNot measured because of solubility limitations.

To gain insight into the origin of the spectroscopic properties observed in solution, the vertical $S_0 \rightarrow S_n$ excitation energies were calculated for the isolated molecules at the time-dependent density functional theory (TD-DFT) level with the B3LYP

functional and the 6-31G** basis set (Table S2, Figures S2 and S3, Supporting Information). The strong low-energy transitions calculated for **2a** and **2b** represent a superposition of $S_0 \rightarrow S_4$ and $S_0 \rightarrow S_5$ in **2a**, and $S_0 \rightarrow S_9$ in **2b**. These transitions are predominantly HOMO-2 \rightarrow LUMO and HOMO-6 \rightarrow LUMO contributions for **2a** and **2b**, respectively; in fact, both the HOMO-2 of **2a** and HOMO-6 of **2b** closely resemble the NDI HOMO (Figure 3). The transitions for **3a** and **3b** correspond to

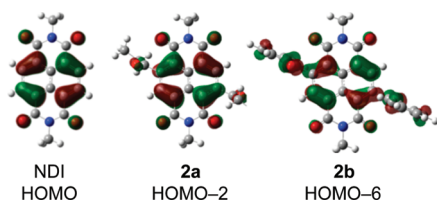


Figure 3. Pictorial representations of the HOMO (-7.04 eV), HOMO-2 (-7.30 eV), and HOMO-6 (-7.27 eV) wave functions for N,N' -dimethyl derivatives of NDI, **2a** ($R = C_2H_5$), and **2b**, respectively, as determined at the B3LYP/6-31G** level of theory (isovalue 0.03).

the $S_0 \rightarrow S_3$ and $S_0 \rightarrow S_2$ transitions, respectively, and are predominantly HOMO \rightarrow LUMO in nature. Accordingly, the bathochromic shifts of the strong transitions of **3a** and **3b** relative to NDI can be attributed to the reduced HOMO-LUMO separation calculated, where both orbitals are destabilized by extension of the NDI core, but with the HOMO being more strongly affected (Table S1, Supporting Information). The additional bathochromic shift seen in **3b** relative to **3a** can be attributed to the reduced HOMO-LUMO separation seen for that compound, which arises from the extension of the HOMO onto the phenyl substituents, as described above.

Cyclic voltammetry (CV) was used to measure the reduction potentials of NDI6, **2a–e**, **3a** and **3b** in $CH_2Cl_2/0.1$ M tBu_4NPF_6 (Table 1, Figures S4 and S5, Supporting Information). Two sequential reversible one-electron reduction processes were observed for each molecule. The half-wave reduction potentials corresponding to reduction to the radical anions ($E_{1/2}^{0/-}$) of **2b–e** are cathodically shifted with increasing fluorine substitution, as expected on the basis of the Hammett parameters³⁴ of the appropriate fluoro-phenyl substituents and consistent with the trend observed in the DFT calculated adiabatic EA values (Table 1). Although more readily reduced NDIs have been reported (notably, a 2,6-dicyano-NDI derivative exhibits a first reduction potential of -0.40 V versus $FeCp_2^{+/0}$ in dichloromethane²³), these ketones are significantly more readily reduced than unsubstituted NDIs, and the potential of **2e** at least falls in the range where stable electron-transport properties might be expected in ambient atmosphere.³⁵ However, the poor π -stacking, low calculated intermolecular couplings, and moderate calculated reorganization energies (vide infra) suggest that electron mobility would be likely to be low.

Both of the hydrazine-fused products, **3a** and **3b** are significantly more difficult to reduce than NDI6, which is consistent with the trends in DFT-calculated LUMO energies and EAs (Tables 1 and S1, Supporting Information). The alkyl-substituted derivative **3a** is ca. 0.10 V less readily reduced than the aryl-substituted derivative **3b**, also consistent with calculations and with the relative inductive properties of alkyl and phenyl groups.³⁴

The intramolecular reorganization energies for a self-exchange electron-transfer reaction between the neutral molecules and the corresponding radical anions, λ_e , were also calculated at the

B3LYP/6-31G** level (Table 1). The calculated λ_e values for all five diacyl-NDI derivatives are on the order of 450 meV, which is significantly larger (by 100 – 140 meV) than that estimated for NDI6. The calculated λ_e values for **3a** and **3b** are smaller by ca. 60 meV than those estimated for NDI6 and are much smaller than the values calculated for the diacyl-NDI derivatives (by ca. 200 meV). For the sake of comparison, λ_e values in a series of 30 PDI derivatives have been calculated to fall in the range 250 – 350 meV.³⁶

Crystal Structure and Electronic Coupling. Crystals of **2b**, **3a**, and **3b** suitable for single-crystal X-ray structure determination were obtained by slow evaporation of a 1:1 solution of dichloromethane and ethyl acetate, slow evaporation of a dichloromethane solution, and liquid-liquid diffusion of a 1,1,2,2-tetrachloroethane-pentanol mixture, respectively (Figure 4).³⁷ Compound **3b** crystallized with the incorporation

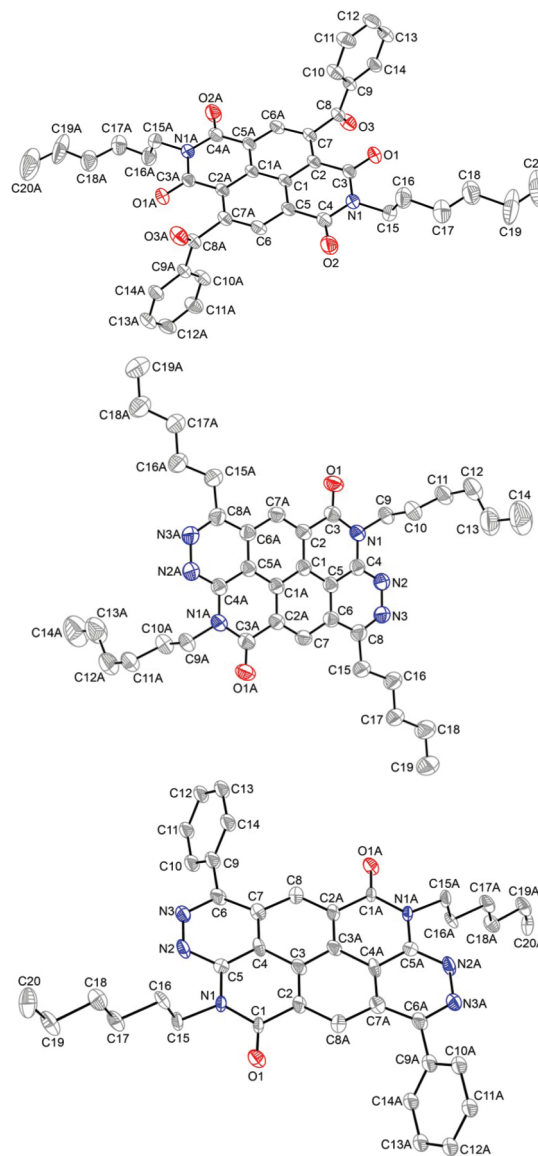


Figure 4. Molecular structures of **2b** (top), **3a** (middle), and **3b** (bottom) determined by X-ray crystallography (50% thermal ellipsoids).

of 1,1,2,2-tetrachloroethane molecules into the lattice; these solvent molecules were found to be severely disordered (details in the Experimental Section). In each case, the conformations of

the molecules (shown in Figure 4) are similar to those found in the calculations on isolated molecules (Figure 1). The packing in the structures are described using pitch and roll angles and distances as described by Curtis et al.³⁸ (Figure S6, Supporting Information), where P and R are the pitch and roll angles corresponding to the molecular slipping along the long (z_L) and short (z_S) axis of the molecule, respectively; d is the π - π distance between two stacked molecular planes; d_P and d_R are the slip distances along the long and short axis, respectively; and d_{tot} is defined as the total slip distance ($d_{\text{tot}} = (d_P^2 + d_R^2)^{1/2}$). These values are summarized for each crystal in Table 2. On the basis

Table 2. Pitch and Roll Angles^a (deg) and Distances^a (Å) along with Electronic Couplings^b (B3LYP/6-31G) between Nearest Pairs (meV) for NDI6, 2b, 3a, and 3b**

compd	P	R	d	d_P	d_R	d_{tot}	t_a	t_b	t_c
NDI6	19.4	45.6	3.3	1.2	3.4	3.6	85	31	0
2b	13.0	47.6	3.8	0.88	4.2	4.3	0	20	0
3a	45.4	11.3	3.3	3.3	0.67	3.4	7	–	–
3b ^c	45.7	18.1	3.3	3.4	1.1	3.6	63	–	0

^aAs defined in the text and respresented by Figure S8, Supporting Information. ^bElectronic couplings calculated along the a - (t_a), b - (t_b), and c - (t_c) axes, respectively, between LUMO levels of pairs of adjacent molecules with intermolecular distances less than 7 Å along the specified axis. ^cC₂H₂Cl₄ solvate.

of the crystal structures of NDI6,³⁹ 2b, 3a, and 3b, the intermolecular effective electronic couplings were evaluated using DFT (Table 2, B3LYP/6-31G**, using the fragment orbital approach⁴⁰).

The X-ray single-crystal structure of NDI6 reported by Shukla et al. was used for comparison purposes.³⁹ The molecular packing in the NDI6 crystal is characterized as a slipped π -stack with close π - π distances ($d = 3.3$ Å) and a total slip distance, d_{tot} , of 3.6 Å resulting in substantial overlap of the NDI cores (Figure 5). The stacks are arranged parallel to one another

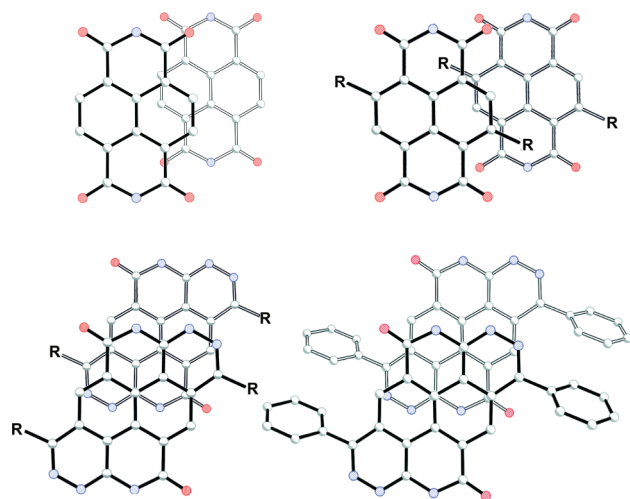


Figure 5. Crystal structure of NDI6 (top left), 2b (top right, R = C(O)C₅H₁₁), 3a (bottom left, R = C₅H₁₁), and 3b (bottom right, C₂H₂Cl₄ solvate) showing the overlap of the cores. N,N' -alkyl groups have been removed for clarity.

(Figure S7, Supporting Information). The LUMO–LUMO electronic couplings (t) for NDI6 were determined to be high for electrons along the a -axis (π - π stacking direction, 85 meV) and relatively low along the b -axis (31 meV); in a tight-binding

approximation, this would provide for a conduction bandwidth along the stacking direction on the order of 350 meV, which is similar to the valence bandwidth in rubrene.⁴¹ These values are comparable to the effective electronic couplings calculated earlier on the basis of the single-crystal structure of N,N' -cyclohexyl-NDI by similar methods (91 and 19 meV for a - and b -axis, respectively).⁴²

Compound 2b also adopts a slipped π -stack structure with much larger π - π and total slip distances when compared to NDI6 (Table 2, Figures 5 and S8, Supporting Information). The large distances observed in 2b are attributed to the aryl-ketone units, which are approximately perpendicular to the plane of the NDI core (the angle between planes formed by the carbon atoms of the NDI and C(O)C of the ketone moiety is 86.5°), consistent with the large torsion angles predicted by DFT. For 2b, the electronic coupling along the π - π stacking direction (b -axis) is determined to be low for electrons (20 meV) compared to that for NDI6, while along the a - and c -axis they are negligible.

Crystals of 3a and 3b (C₂H₂Cl₄ solvate) adopt a slipped π -stack structure with parallel neighboring molecular stacks similar to that observed for NDI6 (Figures 5, S9 and S10, Supporting Information). Although the relative pitch and roll angles and distances are different, the π - π and total slip distances for 3a and 3b are very similar to those measured in the crystal structure of NDI6 (Table 2) and allow for a significant amount of spatial overlap between the cores (Figure 5). However, the core wave function overlap in 3a leads to much smaller electronic couplings than for the solvate of 3b. Unlike the aryl groups of 2b, the aryl moiety in 3b does not impede π - π interactions; the torsion angle between this group and the plane of the core is 60.7°, which is consistent with a decrease in the Ph–core torsion angle calculated for 3b relative to the acyl–core torsion angle calculated for 2b using DFT. Thus, these calculations suggest that, given that 3b displays a significant electronic coupling along the stacking direction (leading to an estimated conduction bandwidth of ~250 meV) and a relatively low reorganization energy, the electron mobility in this compound could be substantial along the a -axis.

CONCLUSION

2,6-Diacyl-NDIs have been synthesized for the first time from the reaction of a 2,6-distannyl NDI and acyl halides, and two examples have been converted to the first examples of the PPP fused-ring system. The new compounds have been characterized by quantum-chemical calculations, UV–vis spectroscopy, cyclic voltammetry, and, in some cases, X-ray crystallography. The redox potentials of these materials can be easily tuned through varying core substitution, with the use of electron-poor acyl-halide coupling partners leading to particularly readily reduced examples. This general synthetic method can potentially be applied in a variety of NDI systems to develop new diacyl-NDI and fused-ring NDI derivatives.

EXPERIMENTAL SECTION

General Experimental Methods. Starting materials were reagent grade and were used without further purification unless otherwise indicated. Anhydrous toluene was obtained by passing through columns of activated alumina. All Stille coupling reactions were performed using oven-dried glassware under nitrogen atmosphere. Chromatographic separations were performed using standard flash column chromatography methods. Electrochemical measurements were carried out under nitrogen in dry deoxygenated 0.1 M tetra-*n*-butylammonium hexafluorophosphate in dichloromethane using a conventional three-electrode cell with a glassy carbon working electrode, platinum wire counter electrode, and a Ag wire coated with AgCl as pseudoreference

electrode. Potentials were referenced to $\text{FeCp}_2^{+/0}$ by using ferrocene as an internal reference. Cyclic voltammograms were recorded at a scan rate of 50 mV s^{-1} . UV–vis spectra were recorded in 1 cm cells in dichloromethane solvents. Melting points were measured using differential scanning calorimetry (DSC) at a scanning rate of $5 \text{ }^\circ\text{C min}^{-1}$.

X-ray Diffraction. Crystals of **2b**, **3a**, and **3b** suitable for single-crystal X-ray structure determination were obtained by slow evaporation of a 1:1 solution of dichloromethane and ethyl acetate, slow evaporation of a dichloromethane solution, and liquid–liquid diffusion of a 1,1,2,2-tetrachloroethane–pentanol mixture, respectively.

The X-ray diffraction data were collected at 100 K using graphite monochromated Mo $K\alpha$ radiation ($\lambda = 0.71073 \text{ \AA}$). Absorption corrections were applied semiempirically using APEX2 program.⁴³ The structures were solved by direct methods and refined by full matrix least-squares on F^2 in the anisotropic approximation for non-hydrogen atoms. The phenyl ring of molecule **3b** was found to be disordered over two positions with the occupancies 0.51/0.49. For the final refinement, the contribution of a severely disordered 1,1,2,2-tetrachloroethane molecule of crystallization was removed from the diffraction data with PLATON⁴⁴/SQUEEZE.⁴⁵ All hydrogen atom positions were refined in isotropic approximation in “riding” model with the $U_{\text{iso}}(\text{H})$ parameters equal to $1.2 U_{\text{eq}}(\text{C}_i)$, for methyl groups equal to $1.5 U_{\text{eq}}(\text{C}_i)$, where $U(\text{C}_i)$ and $U(\text{C}_i)$ are respectively the equivalent thermal parameters of the carbon atoms to which the corresponding H atoms are bonded. Data reduction and further calculations were performed by using the SHELXS-97⁴⁶ and SHELXL-97⁴⁷ (**2b** and **3a**) or SHELXTL⁴⁸ (**3b**) program packages. Selected refinement data and structure parameters are shown in Table S3, Supporting Information.

Computational Methodology. Calculations for the isolated (neutral, radical-cation, and radical-anion) molecules in their electronic ground state were carried out at the density functional theory (DFT) level, using B3LYP hybrid,^{49–51} a global hybrid functional, in conjunction with a 6-31G**^{52–54} basis set. All N,N' -alkyl groups were replaced with methyl groups, and all alkyl R groups were replaced with ethyl groups to reduce the computational cost. The optimized geometries are true minima with no imaginary harmonic vibrational frequencies. All calculations were performed using the Gaussian (03 revision E.01⁵⁵ and 09 revision A.02⁵⁶) suite of programs.

General Procedure for Preparation of Compounds 2a–e. A solution of **1**²⁹ (1 equiv), acylchloride (2–3 equiv), and copper(I) iodide (10 mol %) in dry toluene (0.05 M wrt **1**) was deoxygenated with nitrogen for 5 min. Dichloro-bis(triphenylphosphine)palladium (5 mol %) was added, and the reaction mixture was heated to $100 \text{ }^\circ\text{C}$ for 1.5–4 h.

N,N' -Di(*n*-hexyl)-2,6-dihexanoylnaphthalene-1,8:4,5-bis(dicarboximide), 2a. This compound was synthesized according to the general procedure using **1** (1.98 mmol), hexanoyl chloride (5.93 mmol), CuI (0.198 mmol), Pd(PPh₃)₂Cl₂ (0.099 mmol), and toluene (40 mL). After cooling, the reaction mixture was filtered through a plug of Celite eluting with toluene, and the filtrate was concentrated via rotary evaporation. The crude product was purified by flash chromatography (silica gel, 0–2% methanol in dichloromethane). The product was recrystallized twice from ethyl acetate and collected as a white solid (0.333 g, 0.518 mmol, 26%, mp $262 \text{ }^\circ\text{C}$). ¹H NMR (400 MHz, CDCl₃) δ 8.46 (s, 2H), 4.11 (t, $J = 7.6 \text{ Hz}$, 4H), 2.86 (t, $J = 7.4 \text{ Hz}$, 4H), 1.85 (quint., $J = 7.4 \text{ Hz}$, 4H), 1.66 (quint., $J = 7.5 \text{ Hz}$, 4H), 1.50–1.20 (m, 20H), 0.92 (t, $J = 7.0 \text{ Hz}$, 6H), 0.87 (t, $J = 6.9 \text{ Hz}$, 6H). ¹³C{¹H} NMR (100 MHz, CDCl₃) δ 205.0, 162.2, 161.8, 146.9, 129.4, 126.9, 126.4, 122.2, 43.2, 41.2, 31.4, 31.3, 27.9, 26.6, 23.4, 22.5, 22.4, 14.0, 13.9. HRMS (EI) m/z calcd for C₃₈H₅₁N₂O₆ (M^+), 630.3669; found, 630.3674. Anal. Calcd. for C₃₈H₅₀N₂O₆: C, 72.35; H, 7.99; N, 4.44. Found: C, 72.65; H, 7.94; N 4.47. IR (KBr) ν 3058 (w), 2958, 2930, 2872, 1697 (s), 1652 (s), 1453, 1381, 1324, 1182, 1149, 798, 768 cm^{-1} .

N,N' -Di(*n*-hexyl)-2,6-dibenzoylnaphthalene-1,8:4,5-bis(dicarboximide), 2b. This compound was synthesized according to the general procedure using **1** (1.98 mmol), hexanoyl chloride (5.93 mmol), CuI (0.198 mmol), Pd(PPh₃)₂Cl₂ (0.099 mmol), and toluene (40 mL). After cooling, the reaction mixture was filtered through a plug of Celite eluting with toluene, and the filtrate was concentrated via rotary evaporation. The crude product was purified by

flash chromatography (silica gel, 0–2% methanol in dichloromethane). The product was recrystallized twice from ethyl acetate and collected as a white solid (0.376 g, 0.596 mmol, 30%, mp $327 \text{ }^\circ\text{C}$). ¹H NMR (400 MHz, CDCl₃) δ 8.63 (s, 2H), 7.79 (d, $J = 7.3 \text{ Hz}$, 4H), 7.62 (t, $J = 7.4 \text{ Hz}$, 2H), 7.47 (t, $J = 7.8 \text{ Hz}$, 4H), 4.02 (t, $J = 7.1 \text{ Hz}$, 4H), 1.59 (m, 4H), 1.33–1.15 (m, 12H), 0.81 (t, $J = 6.9 \text{ Hz}$, 6H). ¹³C{¹H} NMR (100 MHz, CDCl₃) δ 194.8, 161.8, 161.7, 145.0, 135.5, 134.1, 130.6, 129.2, 128.9, 126.8, 126.6, 123.9, 41.2, 31.3, 27.8, 26.5, 22.4, 13.9. HRMS (EI) m/z calcd for C₄₀H₃₉N₂O₆ (M^+), 642.2730; found, 642.2741. Anal. Calcd. for C₄₀H₃₈N₂O₆: C, 74.75; H, 5.96; N, 4.36. Found: C, 74.49; H, 5.85; N 4.29. IR (KBr) ν 3063 (w), 2962, 2926, 2853, 1708 (s), 1679 (s, br), 1583, 1450, 1347, 1315, 1225, 1196, 1130, 861, 793, 686 cm^{-1} .

N,N' -Di(*n*-hexyl)-2,6-bis(4-fluorobenzoyl)naphthalene-1,8:4,5-bis(dicarboximide), 2c. This compound was synthesized according to the general procedure using **1** (0.490 mmol), hexanoyl chloride (1.04 mmol), CuI (0.020 mmol), Pd(PPh₃)₂Cl₂ (0.010 mmol), and toluene (5 mL). After cooling, the reaction mixture was filtered through a plug of Celite eluting with toluene, and the filtrate was concentrated via rotary evaporation. The crude product was purified by flash chromatography (silica gel, 0–1% ethyl acetate in chloroform). The product was recrystallized twice from ethyl acetate and collected as a white solid (0.106 g, 0.156 mmol, 32%, mp $306 \text{ }^\circ\text{C}$). ¹H NMR (400 MHz, CDCl₃) δ 8.61 (s, 2H), 7.81 (dd, $J_{\text{HF}} = 5.2$, $J_{\text{HH}} = 8.8 \text{ Hz}$, 4H), 7.14 (apparent t, $J_{\text{HF}} \sim J_{\text{HH}} \sim 8.6 \text{ Hz}$, 4H), 4.02 (t, $J = 7.3 \text{ Hz}$, 4H), 1.67–1.53 (m, 4H), 1.35–1.13 (m, 12H), 0.82 (t, $J = 6.9 \text{ Hz}$, 6H). ¹³C{¹H} NMR (100 MHz, CDCl₃) δ 193.2, 166.3 (d, $J_{\text{CF}} = 255 \text{ Hz}$), 161.7, 161.6, 144.7, 132.1, 131.9, 131.8, 130.5, 126.8 (d, $J_{\text{CF}} = 20 \text{ Hz}$), 123.5, 116.2 (d, $J_{\text{CF}} = 22 \text{ Hz}$), 41.2, 31.3, 27.8, 26.5, 22.4, 13.9. ¹⁹F NMR (375 MHz, CDCl₃, referenced to (trifluoromethyl)benzene in CDCl₃) δ –104.15 (s). HRMS (EI) m/z [M^+] calcd for C₄₀H₃₆F₂N₂O₆ 678.2541; found, 678.2557. Anal. Calcd. for C₄₀H₃₆F₂N₂O₆: C, 70.78; H, 5.35; N, 4.13. Found: C, 70.55; H, 5.42; N 4.09. IR (KBr) ν 3069 (w), 2965, 2929, 2860, 1708 (s), 1657 (s, br), 1598, 1507, 1450, 1317, 1225, 1154, 849, 618, 509 cm^{-1} .

N,N' -Di(*n*-hexyl)-2,6-bis(4-(trifluoromethyl)benzoyl)naphthalene-1,8:4,5-bis(dicarboximide), 2d. This compound was synthesized according to the general procedure using **1** (0.490 mmol), hexanoyl chloride (1.04 mmol), CuI (0.020 mmol), Pd(PPh₃)₂Cl₂ (0.010 mmol), and toluene (5 mL). After cooling, the reaction mixture was diluted with 1,1,2,2-tetrachloroethane and filtered through a plug of silica gel eluting with 1,1,2,2-tetrachloroethane and ethyl acetate. The filtrate was diluted with hexanes and placed at $-20 \text{ }^\circ\text{C}$ for 1 h to precipitate a white solid. The crude product was recrystallized from dichloromethane and collected as a white solid (0.112 mg, 0.144 mmol, 29%, mp $347 \text{ }^\circ\text{C}$). ¹H NMR (400 MHz, C₂D₂Cl₄) δ 8.64 (s, 2H), 7.92 (d, $J = 8.0 \text{ Hz}$, 4H), 7.76 (d, $J = 8.3 \text{ Hz}$, 4H), 4.03 (t, $J = 7.3 \text{ Hz}$, 4H), 1.70–1.50 (m, 4H + H₂O overlap), 1.35–1.15 (m, 12H), 0.83 (t, $J = 6.6 \text{ Hz}$, 6H). ¹⁹F NMR (375 MHz, C₂D₂Cl₄, referenced to (trifluoromethyl)benzene in CDCl₃) δ –62.94 (s). HRMS (EI) m/z calcd for C₄₂H₃₆F₆N₂O₆ (M^+), 778.2478; found, 778.2477. Anal. Calcd. for C₄₂H₃₆F₆N₂O₆: C, 64.78; H, 4.66; N, 3.60. Found: C, 64.58; H, 4.54; N 3.59. IR (KBr) ν 3067 (w), 2962, 2932, 2859, 1710 (s), 1685 (s, br), 1659, 1452, 1328, 1225, 1132, 1068, 855 cm^{-1} . A ¹³C NMR spectrum was not obtained because of the poor solubility of **2d**.

N,N' -Di(*n*-hexyl)-2,6-bis(3,4,5-trifluorobenzoyl)naphthalene-1,8:4,5-bis(dicarboximide), 2e. This compound was synthesized according to the general procedure using **1** (0.490 mmol), hexanoyl chloride (1.04 mmol), CuI (0.020 mmol), Pd(PPh₃)₂Cl₂ (0.010 mmol), and toluene (5 mL). After cooling, the reaction mixture was diluted with 1,1,2,2-tetrachloroethane and filtered through a plug of Celite. The solvent was removed under reduced pressure. The crude product was recrystallized from chlorobenzene and collected as a white solid (0.034 mg, 0.045 mmol, 9.2%, mp $350 \text{ }^\circ\text{C}$). ¹H NMR (400 MHz, C₂D₂Cl₄) δ 8.62 (s, 2H), 7.45 (m, 4H), 4.04 (m, 4H), 1.70–1.50 (m, 4H + H₂O overlap), 1.40–1.20 (m, 12H), 0.85 (m, 6H). ¹⁹F NMR (375 MHz, C₂D₂Cl₄, referenced to (trifluoromethyl)benzene in CDCl₃) δ –68.05 (d, $J = 18.8 \text{ Hz}$, 2F), –87.07 (m, 4F). HRMS (EI) m/z calcd for C₄₀H₃₂F₆N₂O₆ (M^+), 750.2165; found, 750.2150. Anal. Calcd. for C₄₀H₃₂F₆N₂O₆: C, 64.00; H, 4.30; N, 3.73. Found: C, 63.72; H, 4.34; N 3.79. IR (KBr) ν 3072, 2961, 2926, 2859, 1715 (s), 1668 (s, br), 1529,

1446, 1355, 1314, 1193, 1043, 736 cm^{-1} . A ^{13}C NMR spectrum was not obtained because of the poor solubility of **2e**.

1,7-Di(*n*-pentyl)-4,10-di(*n*-hexyl)phthalazino[6,7,8,1-*lmna*]-pyridazino[5,4,3-*gh*][3,8]phenanthroline-5,11(4*H*,10*H*)-dione, **3a.** To a solution of **2a** (0.200 g, 0.317 mmol) in ethanol (6 mL) at 80 °C was added hydrazine monohydrate (0.5 mL). The reaction mixture was heated at 100 °C in a pressure tube for 2 days while being monitored by TLC. After cooling, the reaction mixture was diluted with dichloromethane and filtered. The solvent was removed under reduced pressure. The crude product was purified by flash chromatography (silica gel, 0–3% methanol in dichloromethane). The product was recrystallized from dichloromethane and twice from methanol to yield yellow crystals (0.073 g, 0.117 mmol, 37%, mp 136 °C). ^1H NMR (400 MHz, CDCl_3) δ 9.47 (s, 2H), 4.86 (t, $J = 7.6$ Hz, 4H), 3.65 (t, $J = 7.8$ Hz, 4H), 2.08 (quint., $J = 7.6$ Hz, 4H), 1.97 (quint., $J = 7.6$ Hz, 4H), 1.60–1.50 (m, 8H), 1.50–1.25 (m, 12H), 0.93 (t, $J = 7.2$ Hz, 6H), 0.88 (t, $J = 7.1$ Hz, 6H). $^{13}\text{C}\{^1\text{H}\}$ NMR (100 MHz, CDCl_3) δ 160.6, 157.4, 149.7, 128.3, 125.7, 124.4, 123.3, 110.9, 42.4, 33.3, 31.8, 31.6, 29.4, 27.8, 26.8, 22.6, 22.5, 14.0, 13.9. HRMS (MALDI) m/z calcd for $\text{C}_{38}\text{H}_{51}\text{N}_6\text{O}_2$ (MH^+), 623.4034; found, 623.4074. Anal. Calcd. for $\text{C}_{38}\text{H}_{50}\text{N}_6\text{O}_2$: C, 73.28; H, 8.09; N, 13.49. Found: C, 72.69; H, 7.97; N 13.63. IR (KBr) ν 2958, 2927, 2860, 1680 (s), 1457, 1413, 1270, 761 cm^{-1} . We were unable to obtain an elementally pure sample of **3a** (C analysis differs from calculated value by 0.6%); however, the reported ^1H NMR spectrum (Supporting Information) and X-ray crystal structure of **3a** indicate essential purity of the sample and formation of the desired structure, respectively.

4,10-Di(*n*-hexyl)-1,7-diphenylphthalazino[6,7,8,1-*lmna*]-pyridazino[5,4,3-*gh*][3,8]phenanthroline-5,11(4*H*,10*H*)-dione, **3b.** To a solution of **2b** (0.200 g, 0.311 mmol) in ethanol (6 mL) at 80 °C was added hydrazine monohydrate (0.2 mL). The reaction mixture was heated at 100 °C in a pressure tube for 2 days while being monitored by TLC. Additional hydrazine monohydrate (0.5 mL) was added, and the reaction was heated at 100 °C for 2 more days while being monitored by TLC. After cooling, the reaction mixture was diluted with chloroform and filtered. The solvent was removed under reduced pressure. The product was purified by flash chromatography (silica gel, 5% ethyl acetate in chloroform). Upon fraction collection, a yellow solid began to precipitate from chloroform solution. The product fraction was placed in the freezer, and the product was collected as a yellow solid (0.069 g, 0.108 mmol, 35%). ^1H NMR (400 MHz, $\text{C}_2\text{D}_2\text{Cl}_4$) δ 9.57 (s, 2H), 7.97 (m, 4H), 7.76 (m, 6H), 4.92 (t, $J = 7.7$ Hz, 4H), 2.01 (quint., $J = 7.7$ Hz, 4H), 1.60–1.50 (m, 4H), 1.50–1.30 (m, 8H), 0.91 (t, $J = 7.2$ Hz, 6H). $^{13}\text{C}\{^1\text{H}\}$ NMR (100 MHz, $\text{C}_2\text{D}_2\text{Cl}_4$) δ 160.5, 156.2, 149.6, 134.9, 130.3, 130.1, 129.2, 128.3, 127.8, 124.1, 123.2, 111.1, 42.5, 31.5, 27.8, 26.8, 22.6, 14.1. HRMS (MALDI) m/z calcd for $\text{C}_{40}\text{H}_{39}\text{N}_6\text{O}_2$ (MH^+), 635.3134; found, 635.3140. Anal. Calcd. for $\text{C}_{40}\text{H}_{38}\text{N}_6\text{O}_2$: C, 75.69; H, 6.03; N, 13.24. Found: C, 75.40; H, 6.04; N 13.08.

■ ASSOCIATED CONTENT

■ Supporting Information

Supporting tables and figures, additional characterization of **2–3**, and X-ray crystallographic data (CIF) of **2b**, **3a**, and **3b**. This material is available free of charge via the Internet at <http://pubs.acs.org>.

■ AUTHOR INFORMATION

Corresponding Author

*E-mail: seth.marder@chemistry.gatech.edu.

Notes

The authors declare the following competing financial interests: S.R.M. and J.L.B. consult for Solvay.

■ ACKNOWLEDGMENTS

We thank Solvay S.A. and the NSF (STC Program, DMR-0120967; PREM Program, DMR-0934212) for support, Chad

Risko for helpful discussion, and Yadong Zhang for DSC measurements.

■ REFERENCES

- Zhan, X.; Facchetti, A.; Barlow, S.; Marks, T. J.; Ratner, M. A.; Wasielewski, M. R.; Marder, S. R. *Adv. Mater.* **2011**, *23*, 268–284.
- Würthner, F.; Stolte, M. *Chem. Commun.* **2011**, *47*, 5109–5115.
- Zhan, X.; Tan, Z.; Zhou, E.; Li, Y.; Misra, R.; Grant, A.; Domercq, B.; Zhang, X.-H.; An, Z.; Zhang, X.; Barlow, S.; Kippelen, B.; Marder, S. R. *J. Mater. Chem.* **2009**, *19*, 5794–5803.
- Shibano, Y.; Imahori, H.; Adachi, C. *J. Phys. Chem. C* **2009**, *113*, 15454–15466.
- Wei, Y.; Zhang, Q.; Jiang, Y.; Yu, J. *Macromol. Chem. Phys.* **2009**, *210*, 769–775.
- Sadrai, M.; Hadel, L.; Sauers, R. R.; Husain, S.; Krogh-Jespersen, K.; Westbrook, J. D.; Bird, G. R. *J. Phys. Chem.* **1992**, *96*, 7988–7996.
- O’Neil, M. P.; Niemczyk, M. P.; Svec, W. A.; Gosztola, D.; Gaines, G. L.; Wasielewski, M. R. *Science* **1992**, *257*, 63–65.
- Law, K. Y. *Chem. Rev.* **1993**, *93*, 449–486.
- Schenning, A. P. H. J.; von Herrickhuyzen, J.; Jonkheijm, P.; Chen, Z.; Würthner, F.; Meijer, E. W. *J. Am. Chem. Soc.* **2002**, *124*, 10252–10253.
- An, Z.; Odom, S. A.; Kelley, R. F.; Huang, C.; Zhang, X.; Barlow, S.; Padilha, L. A.; Fu, J.; Webster, S.; Hagan, D. J.; Van Stryland, E. W.; Wasielewski, M. R.; Marder, S. R. *J. Phys. Chem. A* **2009**, *113*, 5585–5593.
- Fukuzumi, S.; Ohkubo, K.; Ortiz, J.; Gutiérrez, A. M.; Fernández-Lázaro, F.; Sastre-Santos, Á. *Chem. Commun.* **2005**, 3814–3816.
- Di Antonio, M.; Doria, F.; Richter, S. N.; Bertipaglia, C.; Mella, M.; Sissi, C.; Palumbo, M.; Freccero, M. *J. Am. Chem. Soc.* **2009**, *131*, 13132–13141.
- Gunaratnam, M.; la Fuente, de, M.; Hampel, S. M.; Todd, A. K.; Reszka, A. P.; Schätzlein, A.; Neidle, S. *Bioorg. Med. Chem.* **2011**, *19*, 7151–7157.
- Huang, C.; Barlow, S.; Marder, S. R. *J. Org. Chem.* **2011**, *76*, 2386–2407.
- Jones, B. A.; Facchetti, A.; Wasielewski, M. R.; Marks, T. J. *J. Am. Chem. Soc.* **2007**, *129*, 15259–15278.
- Battagliarin, G.; Zhao, Y.; Li, C.; Müllen, K. *Org. Lett.* **2011**, *13*, 3399–3401.
- Bullock, J. E.; Vagnini, M. T.; Ramanan, C.; Co, D. T.; Wilson, T. M.; Dicke, J. W.; Marks, T. J.; Wasielewski, M. R. *J. Phys. Chem. B* **2010**, *114*, 1794–1802.
- Molinari, A. S.; Alves, H.; Chen, Z.; Facchetti, A.; Morpurgo, A. F. *J. Am. Chem. Soc.* **2009**, *131*, 2462–2463.
- Nolde, F.; Pisula, W.; Müller, S.; Kohl, C.; Müllen, K. *Chem. Mater.* **2006**, *18*, 3715–3725.
- Qian, H.; Negri, F.; Wang, C.; Wang, Z. *J. Am. Chem. Soc.* **2008**, *130*, 17970–17976.
- Thalacker, C.; Röger, C.; Würthner, F. *J. Org. Chem.* **2006**, *71*, 8098–8105.
- Röger, C.; Würthner, F. *J. Org. Chem.* **2007**, *72*, 8070–8075.
- Jones, B. A.; Facchetti, A.; Marks, T. J.; Wasielewski, M. R. *Chem. Mater.* **2007**, *19*, 2703–2705.
- Chopin, S.; Chaignon, F.; Blart, E.; Odobel, F. *J. Mater. Chem.* **2007**, *17*, 4139–4146.
- Bhosale, S. V.; Kalyankar, M. B.; Bhosale, S. V.; Langford, S. J.; Reid, E. F.; Hogan, C. F. *New J. Chem.* **2009**, *33*, 2409–2413.
- Yan, H.; Chen, Z.; Zheng, Y.; Newman, C. R.; Quinn, J. R.; Dötz, F.; Kastler, M.; Facchetti, A. *Nature* **2009**, *457*, 679–686.
- Polander, L. E.; Tiwari, S. P.; Pandey, L.; Seifried, B. M.; Zhang, Q.; Barlow, S.; Risko, C.; Brédas, J.-L.; Kippelen, B.; Marder, S. R. *Chem. Mater.* **2011**, *23*, 3408–3410.
- Hu, Y.; Gao, X.; Di, C.-A.; Yang, X.; Zhang, F.; Liu, Y.; Li, H.; Zhu, D. *Chem. Mater.* **2011**, *23*, 1204–1215.
- Polander, L. E.; Romanov, A. S.; Barlow, S.; Hwang, D. K.; Kippelen, B.; Timofeeva, T. V.; Marder, S. R. *Org. Lett.* **2012**, *14*, 918–921.
- Stille, J. K. *Angew. Chem., Int. Ed. Engl.* **1986**, *25*, 508–523.

- (31) Wharton, C. J.; Wrigglesworth, R. *J. Chem. Soc., Perkin Trans. 1* **1985**, 809–813.
- (32) Warner, C. R.; Walsh, E. J.; Smith, R. F. *J. Chem. Soc.* **1962**, 1232–1234.
- (33) The analogous fused ring derivatives of **2c–e** were not synthesized because of the relatively low solubilities of **2c–e**.
- (34) Hansch, C.; Leo, A.; Taft, R. *Chem. Rev.* **1991**, *91*, 165–195.
- (35) Air-stable electron transport has been observed in materials with reduction potentials > ca. -0.33 V vs SCE (ref 1 and references cited therein), which in the solvent and electrolyte used in our study corresponds to ca. -0.79 V vs $\text{FeCp}_2^{+/0}$ (Connelly, N. G.; Geiger, W. E. *Chem. Rev.* **1996**, *96*, 877–910).
- (36) Delgado, M. C. R.; Kim, E.-G.; Filho, D. A. D. S.; Brédas, J.-L. *J. Am. Chem. Soc.* **2010**, *132*, 3375–3387.
- (37) CCDC-872309, 872310, and 872311 contain the supplementary crystallographic data for **2b**, **3a**, and **3b**, respectively. These data can be obtained free of charge from the Cambridge Crystallographic Data Centre via www.ccdc.cam.ac.uk/data_request/cif.
- (38) Curtis, M. D.; Cao, J.; Kampf, J. W. *J. Am. Chem. Soc.* **2004**, *126*, 4318–4328.
- (39) Shukla, D.; Nelson, S. F.; Freeman, D. C.; Rajeswaran, M.; Ahearn, W. G.; Meyer, D. M.; Carey, J. T. *Chem. Mater.* **2008**, *20*, 7486–7491.
- (40) Valeev, E. F.; Coropceanu, V.; da Silva Filho, D. A.; Salman, S.; Brédas, J.-L. *J. Am. Chem. Soc.* **2006**, *128*, 9882–9886.
- (41) da Silva Filho, D. A.; Kim, E. G.; Brédas, J. L. *Adv. Mater.* **2005**, *17*, 1072–1076.
- (42) Adiga, S. P.; Shukla, D. *J. Phys. Chem. C* **2010**, *114*, 2751–2755.
- (43) *APEX2 Software Package*; Bruker AXS Inc.: Madison, WI, 2005.
- (44) Spek, A. L. *Acta Crystallogr., Sect. D: Biol. Crystallogr.* **2009**, *65*, 148–155.
- (45) van der Sluis, P.; Spek, A. L. *Acta Crystallogr., Sect. A: Found. Crystallogr.* **1990**, *46*, 194–201.
- (46) Sheldrick, G. M. *Acta Crystallogr., Sect. A: Found. Crystallogr.* **1990**, *46*, 467–473.
- (47) Sheldrick, G. M.; Schneider, T. R. *Methods Enzymol.: Macromol. Crystallogr., Part B* **1997**, *277*, 319–343.
- (48) Sheldrick, G. M.; Hauptman, H. A.; Weeks, C. M.; Miller, R.; Uson, I. In *International Tables for Crystallography*; Rossmann, M., Arnold, E., Eds.; Kluwer Academic: Dordrecht/Boston/London, 2001; Vol. F, pp 333–345.
- (49) Becke, A. D. *Phys. Rev. A* **1988**, *38*, 3098–3100.
- (50) Becke, A. D. *J. Chem. Phys.* **1993**, *98*, 5648–5652.
- (51) Lee, C.; Yang, W.; Parr, R. G. *Phys. Rev. B* **1988**, *37*, 785–789.
- (52) Hariharan, P.; Pople, J. A. *Theor. Chim. Acta* **1973**, *28*, 213–222.
- (53) Francl, M. M. *J. Chem. Phys.* **1982**, *77*, 3654–3665.
- (54) Rassolov, V. A.; Pople, J. A.; Ratner, M. A.; Windus, T. L. *J. Chem. Phys.* **1998**, *109*, 1223–1229.
- (55) Frisch, M. J. T.; Schlegel, H. B.; Scuseria, G. E.; Robb, M. A.; Cheeseman, J. R.; Montgomery, J. A., Jr.; Vreven, T.; Kudin, K. N.; Burant, J. C.; Millam, J. M.; Iyengar, S. S.; Tomasi, J.; Barone, V.; Mennucci, B.; Cossi, M.; Scalmani, G.; Rega, N.; Petersson, G. A.; Nakatsuji, H.; Hada, M.; Ehara, M.; Toyota, K.; Fukuda, R.; Hasegawa, J.; Ishida, M.; Nakajima, T.; Honda, Y.; Kitao, O.; Nakai, H.; Klene, M.; Li, X.; Knox, J. E.; Hratchian, H. P.; Cross, J. B.; Bakken, V.; Adamo, C.; Jaramillo, J.; Gomperts, R.; Stratmann, R. E.; Yazyev, O.; Austin, A. J.; Cammi, R.; Pomelli, C.; Ochterski, J. W.; Ayala, P. Y.; Morokuma, K.; Voth, G. A.; Salvador, P.; Dannenberg, J. J.; Zakrzewski, V. G.; Dapprich, S.; Daniels, A. D.; Strain, M. C.; Farkas, O.; Malick, D. K.; Rabuck, A. D.; Raghavachari, K.; Foresman, J. B.; Ortiz, J. V.; Cui, Q.; Baboul, A. G.; Clifford, S.; Cioslowski, J.; Stefanov, B. B.; Liu, G.; Liashenko, A.; Piskorz, P.; Komaromi, I.; Martin, R. L.; Fox, D. J.; Keith, T.; Al-Laham, M. A.; Peng, C. Y.; Nanayakkara, A.; Challacombe, M.; Gill, P. M. W.; Johnson, B.; Chen, W.; Wong, M. W.; Gonzalez, C.; Pople, J. A. *Gaussian 03*, revision E.01; Gaussian, Inc.: Wallingford CT, 2004.
- (56) Frisch, M. J. T.; Schlegel, H. B.; Scuseria, G. E.; Robb, M. A.; Cheeseman, J. R.; Scalmani, G.; Barone, V.; Mennucci, B.; Petersson, G. A.; Nakatsuji, H.; Caricato, M.; Li, X.; Hratchian, H. P.; Izmaylov, A. F.;